Electronic Supplementary Material (ESI) for Journal of Materials Chemistry A.

Supporting Information

Establishing the Criteria and Strategies to Achieve High-Power During Discharge of Li–Air Battery

Arghya Dutta*, Kimihiko Ito, Yoshimi Kubo*

National Institute for Materials Science, 1-1 Namiki, Tsukuba 305-0044, Japan

Email: A. D. : dutta.arghya@nims.go.jp and Y. K. : kubo.yoshimi@nims.go.jp

1. Calculation of Q_{max}

Pore volume of CNT measured by N_2 adsorption measurement (Barrett-Joyner-Halenda (BJH) method, for pores with diameter < 180 nm): 0.41 $cm^3\ g^{-1}$

Pore volume of CNT electrode measured by mercury porosimetry (intrusion volume was considered for pores with diameter 180 nm to 180 µm): 0.30 $cm^3\ g^{-1}$

(Volumes of both carbon paper (CP) and actual CNT+CP electrode were measured and the value of CP was subtracted to get the volume of CNT)

Bulk density of Li_2O_2: 2.31 g cm^{-3}

Hence, total 0.71 cm^3 void can accommodate 0.71 × 2.31 g = 1.64 g Li_2O_2

Faraday's Law: $m = \frac{Q}{F} \times \frac{M}{z}$

(m = mass of Li_2O_2 (1.64 g), Q = charge (C), F = Faraday constant (96485 C mol^{-1}), M = molar mass of Li_2O_2 (45.88 g mol^{-1}), z = number of electrons transferred (2))

Solving the equation gives Q_{max} = 1920 mAh g^{-1} (Normalized to CNT mass)

2. Electrochemically active surface area (ECSA) measurement

ECSA of the carbon electrodes was measured by cyclic voltammetry of symmetric carbon|separator|carbon coin type 2032 cells with 100 μL 1 M LiTFSI/TEGDME electrolyte. At first, the capacitance of the electrode was calculated by using the equation[1]

$$C = \int_{E_1}^{E_2} \frac{i\,(E)dE}{2(E_2\text{-}E_1)mv}$$

where C is the specific capacitance of a single electrode. E_1, E_2 are the lower and upper limits of cut-off potentials for CV respectively, i (E) is the instantaneous current, m is the mass of a single electrode and v is the scan rate of CV. The capacitance was calculated from 500th cycle of CV.

After obtaining the specific capacitance, ECSA of an electrode was calculated from:[2]

$$C = \frac{\varepsilon\,\varepsilon_0 A}{d}$$

where ε is the relative dielectric constant of teraglyme (7.79),[3] ε_0 is the permittivity of vacuum (8.85 X 10^{-12} F m^{-1}), A is the ECSA and d is the electric double layer thickness assumed to be the radius of oxygen molecules (~1.5 Å).

3. Oxygen concentration profile in the porous electrode

Dimensionless oxygen concentration inside the porous electrode was calculated by:

$$C(x) = C_0 \exp\left(-x\,\frac{j}{nFC_0D_{\text{eff}}}\right)$$

where $C(x)$, C_0, j, n and D_{eff} are the concentration of oxygen in the electrode at distance x from electrode-oxygen interface, oxygen solubility in the electrolyte, current density normalized to the ECSA, number of electron in the rate limiting step, and effective diffusion coefficient of oxygen in the electrolyte inside the porous electrode, respectively.

C_0 = 4.43 mM, n = 1 (Considering one electron reduction step ($O_2 + e^- \leftrightarrow O_2^-$) to be kinetically rate limiting), $D_{\text{eff}} = D\varepsilon^{\beta}$ (D = 1.6 X 10^{-7} cm^2 s^{-1}, ε = 0.8, β = 1.5)[2, 4]

Figures

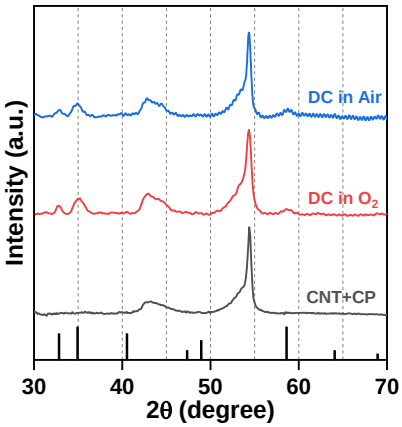

Figure S1. X-ray diffraction (XRD) patterns of the CNT electrodes after discharge in oxygen and air environments up to a capacity of 1.5 mAh at 25 mA g^{-1} DC current. Peak positions for standard Li_2O_2 sample are shown by black vertical lines at the bottom of the plot. XRD of as-prepared CNT electrode is also shown for comparison.

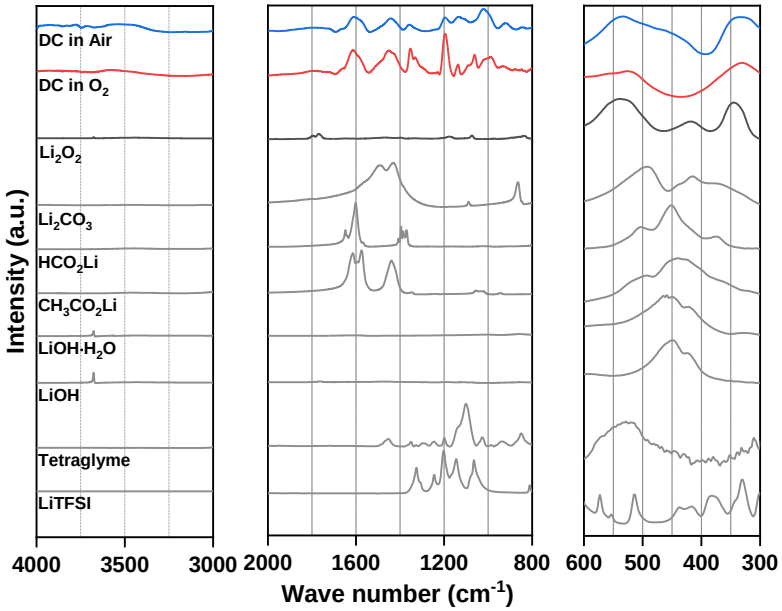

Figure S2. Fourier transform infrared (FTIR) spectra of the CNT electrodes after discharge in oxygen and air environments up to a capacity of 1.5 mAh at 25 mA g^{-1} DC current. Spectra of several lithium salts as potential side products are also shown for comparison.

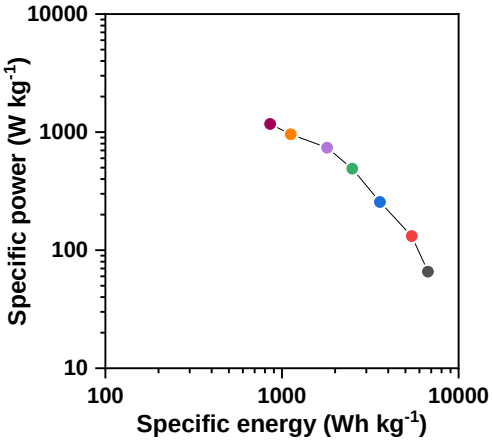

Figure S3. Ragone plot of CNT electrode. Gravimetric energy was calculated by integrating the area below DC curve in Figure 1b) at each current density and gravimetric power was obtained by normalizing gravimetric energy by total DC time at respective current densities. Data points follow same color code as in Figure 1 (b and c).

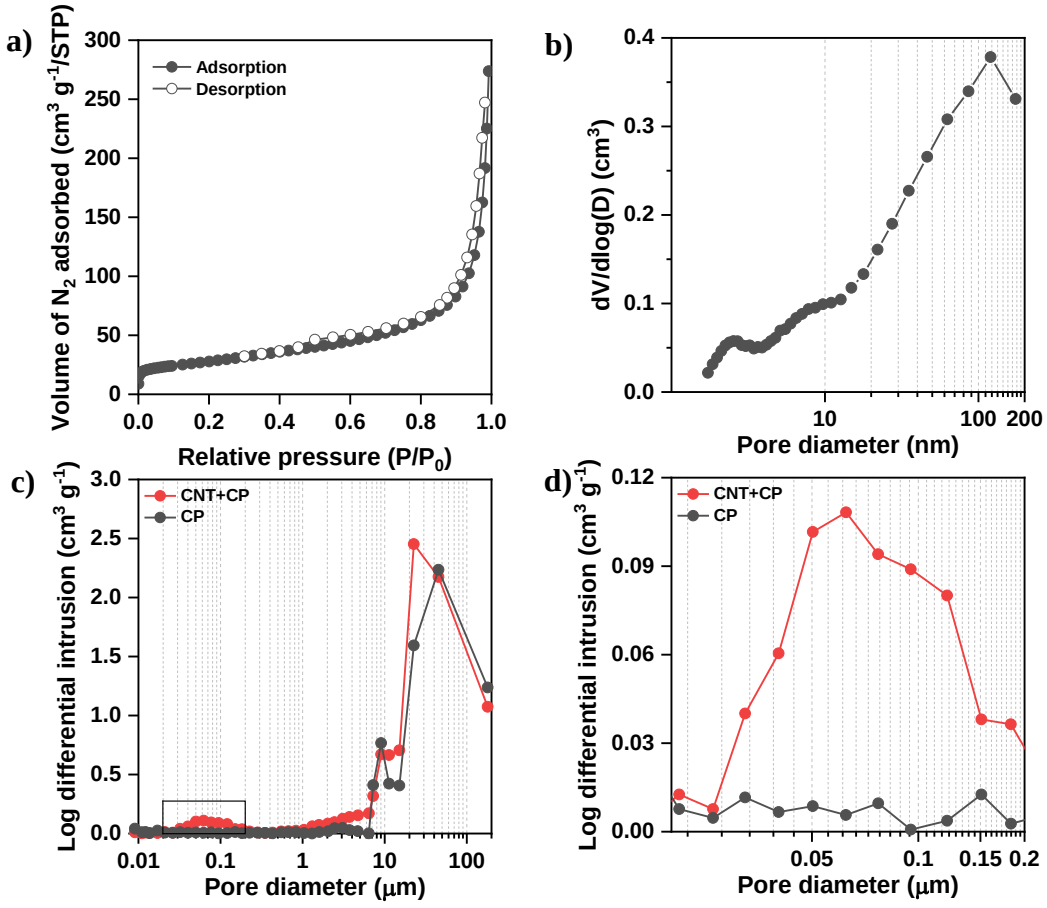

Figure S4. **a)** Nitrogen adsorption/desorption isotherm of CNT powder measured at -196 °C, **b)** Barrett-Joyner-Halenda (BJH) pore-size distribution calculated from nitrogen adsorption measurement, **c)** Pore-size distribution of the actual electrode and the carbon paper (CP, Toray, TGP-H-30) measured by mercury porosimetry. **d)** Magnified part of c) that shows similar pore-size range of BJH pore-size distribution in b).

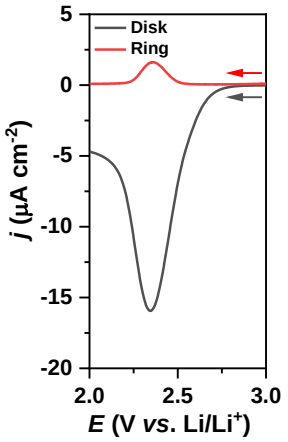

Figure S5. Cathodic linear sweep voltammetry (LSV) with rotating ring disk electrode (RRDE). LSV was carried out with three-electrode cell where glassy carbon was used as both ring and disk electrodes, whereas Li metal was used as counter and reference electrodes in 1 M LiTFSI/TEGDME electrolyte. The potential of the disk was swept from 3 to 2 V *vs*. Li/Li^+ at 0.5 mV s^{-1} and 900 rpm while holding the ring potential at 3.5 V *vs*. Li/Li^+.

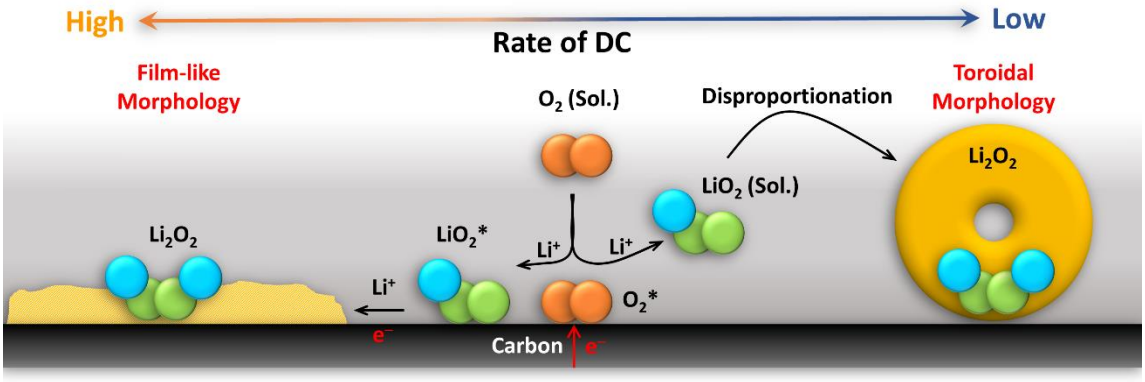

Figure S6. Schematic representation of discharge-rate dependent nucleation and growth of Li_2O_2 in the electrode filled with electrolyte.

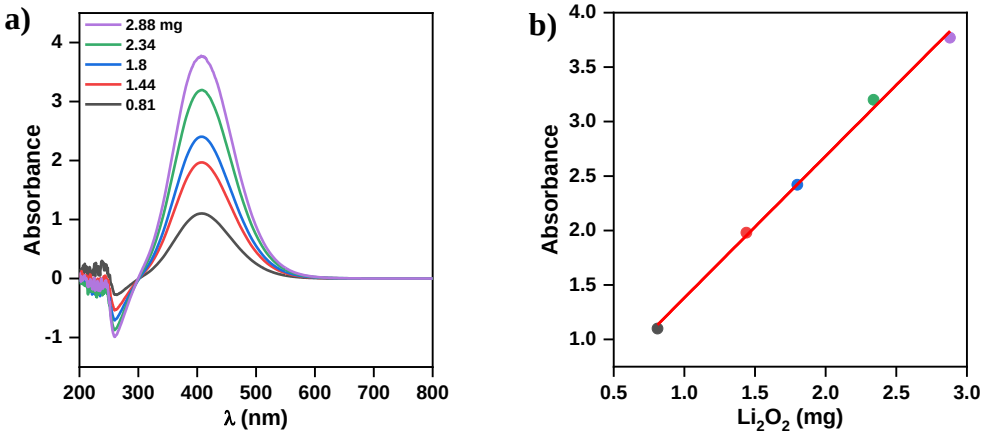

Figure S7. **a)** UV-vis spectra of known amount of commercial Li_2O_2 in $TiOSO_4$ solution. With increase in amount of Li_2O_2 the absorbance of the peak at 407 nm increases gradually due to formation of peroxotitanium complex. Possibly, as the concentration of free $TiOSO_4$ decreases, the absorbance values at wavelengths below the isosbestic point become more negative. **b)** Absorbance (at 407 nm) *vs*. mass of Li_2O_2 calibration curve from a).

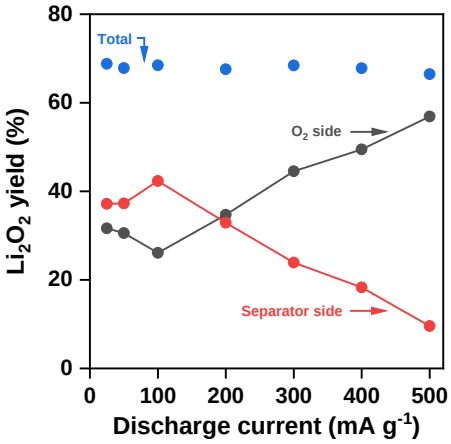

Figure S8. Li_2O_2 yield at different layers of CNT electrodes after DC up to 2 V *vs.* Li/Li^+ as obtained from titration with $TiOSO_4$ solution plotted against current density. Total yield is calculated by adding the values of individual electrodes. The error range for estimation of Li_2O_2 yield was within ±2%.

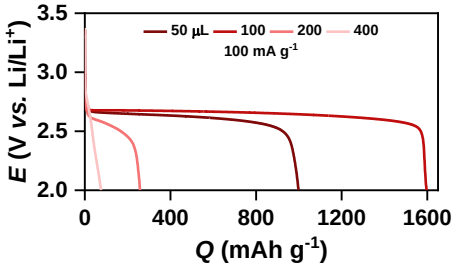

Figure S9. Effect of electrolyte volume on discharge capacity. DC profiles of Li–O_2 cells using single layer CNT electrodes with different volumes of 1 M LiTFSI in TEGDME at 100 mA g^{-1} current density.

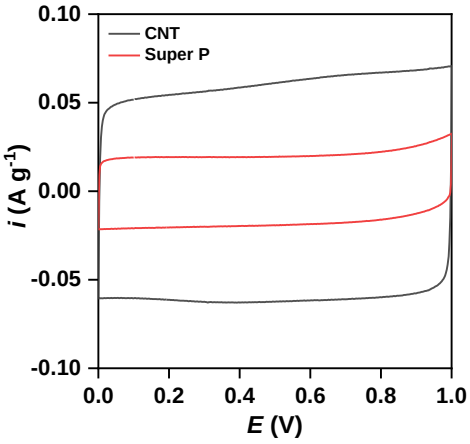

Figure S10. Cyclic voltammetry (500th cycle) of carbon|separator|carbon symmetric cells in the range of 0 to 1 V at 50 mV s^{-1} scan rate. The specific capacitance of CNT and Super P electrodes are calculated to be 2.4 and 0.772 F g^{-1} respectively. Finally, the ECSA of 5.22 m^2 g^{-1} for CNT and 1.68 m^2 g^{-1} for Super P were calculated from these capacitance values.

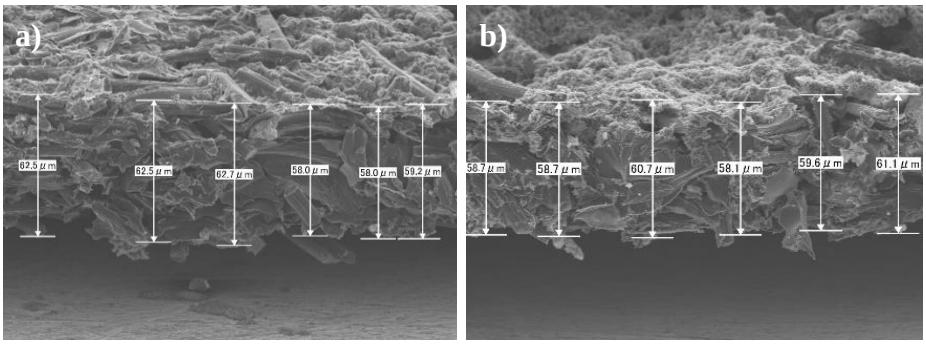

Figure S11. Cross section scanning electron microscopy (SEM) image of **a)** CNT and **b)** Super P electrodes on Toray carbon paper (TGP-H-030). Average thicknesses are calculated to be 60.5 and 59.5 μm for CNT and Super P respectively.

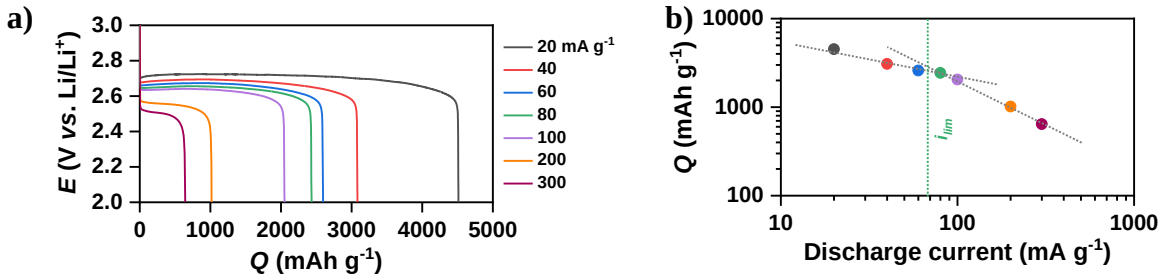

Figure S12. **a)** Discharge profile of Super P electrode cells at different current densities with 1 M LiTFSI in TEGDME up to a cut-off potential of 2 V *vs*. Li/Li$^+$. **b)** Capacity *vs*. DC current plot from a) where dotted green vertical line indicates calculated i_{lim} (69 mA g^{-1}) of Super P electrode.

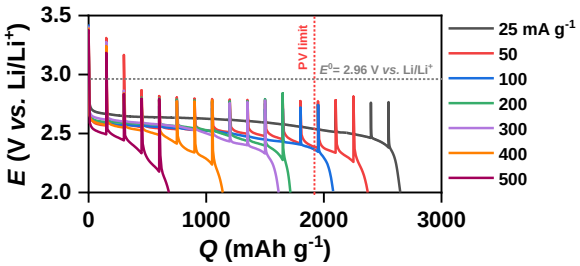

Figure S13. Intermittent current discharge of CNT electrodes in oxygen at different DC currents. Cells were periodically rested for 30 min after every 150 mAh g^{-1} DC up to a cut-off potential of 2 V *vs*. Li/Li$^+$.

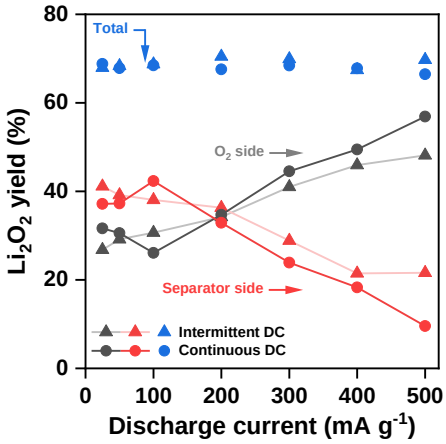

Figure S14. Li_2O_2 yield at different layers of CNT electrodes after DC up to 2 V *vs*. Li/Li^+ with continuous and intermittent current by titrating with $TiOSO_4$ solution. Total yield is calculated by adding the values of individual electrodes. The error range for estimation of Li_2O_2 yield was within ±2%.

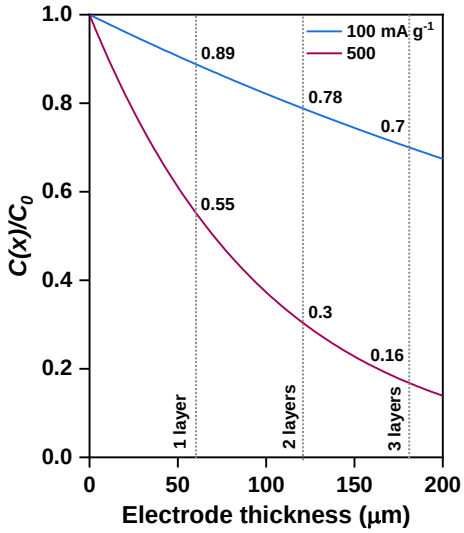

Figure S15. Comparison of dimensionless oxygen concentration at three different depths of the electrode (60.5, 121 and 181.5 μm, marked by vertical dotted lines) corresponding to three layers of CNT at 100 and 500 mA g^{-1} current densities.

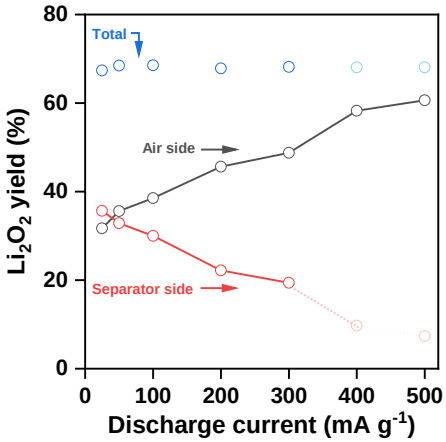

Figure S16. Li_2O_2 yield at different layers of CNT electrodes after DC up to 2 V *vs*. Li/Li^+ in dry air by titrating with $TiOSO_4$ solution. Estimation of Li_2O_2 yield in the layer towards the separator side was not possible at 400 and 500 mA g^{-1} current densities due to negligible amount of Li_2O_2 leading to high error. Values shown in faded red color for 400 and 500 mA g^{-1} are projected by subtracting the yield at the air-side layer from the total average yield (faded blue circles).

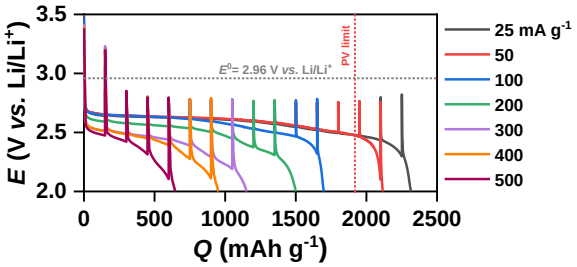

Figure S17. Intermittent current discharge of CNT electrodes at different DC currents in dry air (maximum dew point -60 ºC). Cells were periodically rested for 30 min after every 150 mAh g^{-1} DC up to a cut-off potential of 2 V *vs*. Li/Li^+.

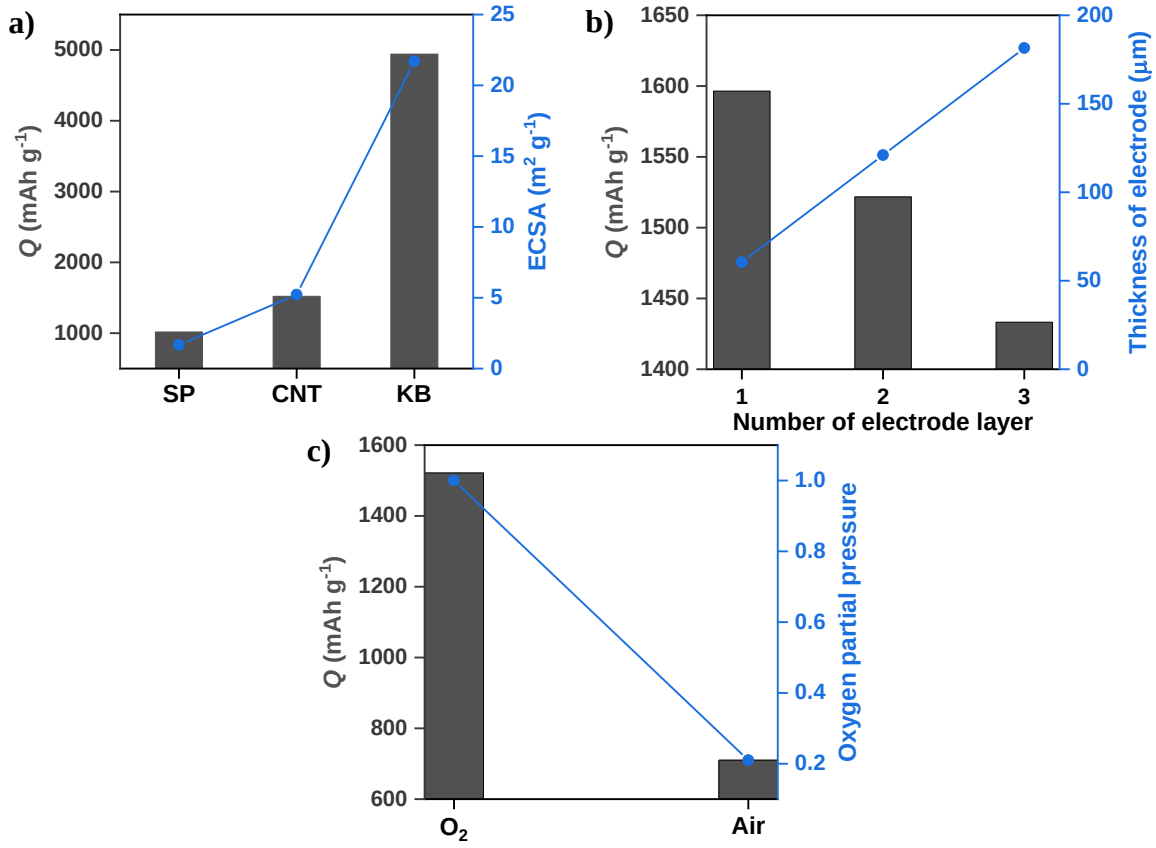

Figure S18. Plots showing relationship between materials properties with specific discharge capacities at a specific current of 100 mA g^{-1}. **a)** Comparison of specific discharge capacities of three carbons super P (SP), carbon nanotube (CNT) and ketjen black (KB) showing increasing trend of capacity with increased ECSA, **b)** Comparison of specific discharge capacities of cells with different thickness of CNT electrodes showing decreasing trend of capacity with increased thickness, and **c)** Comparison of specific discharge capacities of cells in pure oxygen and Air showing decreasing trend of capacity with decreased partial pressure of oxygen.

References

1. W. Chen, Z. Fan, L. Gu, X. Bao, C. Wang, *Chem. Commun.*, 2010, **46**, 3905-3907.

2. F. S. Gittleson, R. E. Jones, D. K. Ward, M. E. Foster, *Energy Environ. Sci.*, 2017, **10**, 1167-1179.

3. C. Wohlfarth, in Static Dielectric Constants of Pure Liquids and Binary Liquid Mixtures, ed. M. D. Lechner, Springer Berlin Heidelberg, Berlin, Heidelberg, 2015; pp 201-201.

4. C. O. Laoire, S. Mukerjee, K. M. Abraham, E. J. Plichta, M. A. Hendrickson, *J. Phys. Chem. C*, 2010, **114**, 9178-9186.